ELSEVIER

Polymer 41 (2000) 6395–6402

polymer

Mechanical properties and phase behaviour of poly(dimethylsilylene-*co*-methyl-*n*-propylsilylene)

A. Kaito*, H. Kyotani, N. Tanigaki, M. Wada, M. Yoshida

Department of Polymer Physics, National Institute of Materials and Chemical Research, 1-1 Higashi, Tsukuba, Ibaraki 305-8565, Japan

Received 9 July 1999; received in revised form 4 October 1999; accepted 9 November 1999

Abstract

The mechanical properties and the phase behaviour of poly(dimethylsilylene-*co*-methyl-*n*-propylsilylene) (PDM-*co*-MPS), were investigated by the measurements of dynamic viscoelasticity, wide angle X-ray diffraction, thermal analysis and UV spectrum. PDM-*co*-MPS was soluble in common organic solvents if the ratio of dimethylsilylene (DM) unit to methyl-*n*-propylsilylene (MP) unit, DM/MP, was lower than 70/30. The crystal phase was transformed into the columnar mesophase above 80–90°C, and the disordering of conformation and the orientation relaxation proceeded with further rise in temperature in the range of 80–130°C. The PDM-*co*-MPS films were extensible only in the narrow temperature range, in which the crystal to mesophase transition started to occur, because the structural relaxation in the columnar mesophase reduced the extensibility of the PDM-*co*-MPS films. The oriented films of PDM-*co*-MPS were prepared by stretching the solution-cast films at 70–80°C to a draw ratio of 7–8. The elastic modulus was much improved in the hot drawn film relative to that of the isotropic films, and the increase of modulus was related to the high degree of orientation in the crystal phase. A large loss tan δ was observed at −20 to −10°C, and the dynamic storage modulus markedly decreased with the rise in temperature in the range of this transition. As the low temperature transition was not detected in the DSC and spectroscopic measurements, it would be assigned to the local molecular motion of the *n*-propyl side group and/or to the glass transition.

Keywords: Polysilane; Mechanical properties; Phase behaviour

1. Introduction

Polysilanes have received the attention of researchers because of their unique electronic and optical properties, which originated from the delocalization of σ-electrons along the main-chains [1,2]. These polymers are expected to have various potential applications including photoresists [3,4], electron conductive circuit [5,6], electroluminescence devise [7–10], photoconductive layer in photo-copiers, and so on. Although the electronic and optical properties of polysilanes have been extensively studied in the past, few works have been reported on the mechanical properties of polysilanes, which seem to be important in some application fields. The elastic modulus and fracture strain were investigated on a series of poly(*n*-pentyl-*n*-alkylsilanes) [11]. These polysilane films are shown to be extensible in the condis crystalline columnar mesophases. We have evaluated the crystal modulus of poly(dimethylsilylene) (PDMS) in the direction of molecular chain-axis from the frequency of the longitudinal acoustic mode, which is observed in the low wavenumber region of the Raman scattering of a series of oligosilanes [12]. Hot drawing is one of the most important methods for the processing of uniaxially oriented films in which the mechanical properties are improved in the drawing direction. It is however not easy to prepare the free-standing films of highly oriented polysilane by hot drawing, because polysilane films are generally brittle and are fractured only at a small strain. The only reported study on this subject is that the free standing films of poly(methylethylsilylene) with high molecular weight were successfully stretched to a draw ratio higher than 10 [13].

The attempt to improve the mechanical properties of polysilanes falls in a dilemma. A film of polysilane having long alkyl side-chains is not extensible to a high strain and expected to be weak, because the long side-chain cannot be a stress-transmitter. On the contrary, polysilanes with short side-groups cannot be processed into materials owing to the poor solubility in organic solvents. One of the clues to the problem is to use a copolymer of polysilane, because disordered molecular structure would depress the crystallization and thereby enhance the solubility. Polydimethylsilylene is a highly crystalline polymer that is not soluble at room

* Corresponding author. Tel.: +81-298-54-6395; fax: +81-298-54-6232.
E-mail address: kaito@home.nimc.go.jp (A. Kaito).

0032-3861/00/$ - see front matter
PII: S0032-3861(99)00841-1

Table 1
Molecular weight and composition of PDM-*co*-MPS

Monomer feed ratio (DM/MP)	Measured composition	M_w	M_n
50/50	58/42	279,000	98,000
60/40	63/37	340,000	84,000
70/30	69/31		9900
80/20	78/22		8200

temperature and does not melt before decomposition. It was reported that copolymerization of methyl-ethylsilylene or methyl-*n*-propylsilylene units into the dimethylsilylene (DM) unit leads to tractable polymers that are soluble in common solvents at ambient temperature [14]. Various copolymers of polyalkylsilanes were synthesized and their phase behaviours were discussed in relation to their random sequence distribution [15–19].

In this work, we tried to prepare highly extensible films of polysilanes using poly(dimethylsilylene-*co*-methyl-*n*-propylsilylene) (PDM-*co*-MPS). The DM units are expected to enhance the mechanical properties, and methyl-*n*-propylsilylene (MP) units would improve the solubility. The phase behaviour of the PDM-*co*-MPS films was investigated by thermal analysis, dynamic viscoelasticity and spectroscopic measurements, and was discussed in relation to the extensibility of the films. The highly oriented films PDM-*co*-MPS were prepared by stretching the film at elevated temperature, and their mechanical properties were studied in connection with the orientation development.

2. Experimental

2.1. Materials

PDM-*co*-MPS was prepared by the sodium-mediated Wurtz coupling reaction of the corresponding dichlorosilanes. The monomers were purified by vacuum-distillation. The reaction was carried out at 111°C in refluxing toluene under Ar atmosphere. Pouring the solution into ethanol solidified the white powder, after the reaction mixture was filtered. The solution of the powder was washed with water for several times in order to remove the salt. Molecular weight distribution was measured using a gel permeation chromatography (GPC) equipment calibrated with polystyrene standards. The bimodal molecular weight distribution was observed on the GPC curve of the copolymers, and the higher molecular weight fraction was fractionated by the repeated reprecipitation from hexane solution with 2-propanol. The molecular weight of the sample is summarized in Table 1. The composition of the copolymers was determined by the ^{1}H NMR spectroscopy. The relative intensity of the ^{1}H NMR signals of C–CH_3 group and Si–CH_3 group was used to evaluate the composition ratio. The measured ratio of DM to MP units (DM/MP) is slightly higher than the feed ratio. If the DM/MP ratio is above 63/37, the copolymer does not dissolve in common organic solvents except for the low molecular weight fraction (M_n = 8000–10, 000). The higher molecular weight fractions of the 58/42 and 63/37 (DM/MP) copolymers were used for the experiment.

The polysilane films 20–40 μm thick were prepared by casting the hexane solution of PDM-*co*-MP on a flat glass plate. Transparent films were obtained after the solvent was slowly evaporated. The films were cut into strips 3 mm wide and 20 mm long, which were stretched at a constant strain rate of 100%/min. They could be stretched reproducibly only in the narrow temperature range (65–80°C). A neck formed on the film at the initial stage of drawing, and gradually propagated in the drawing process. The films fractured immediately after the neck-propagation was completed. The natural draw ratio of the films is 7–8, and it is difficult to control the draw ratio.

2.2. Characterization

The differential scanning calorimetry (DSC) was measured at a heating rate of 20 K/min with a Perkin–Elmer DSC 7 differential scanning calorimeter calibrated with indium. The dynamic viscoelasticity was measured on a dynamic viscoelastometer, Rheovibron DDV-II-EA (Orientec Co. Ltd). The dynamic tensile strain with an amplitude of 2 μm and a frequency of 35 Hz was applied to the rectangular specimens 2 mm wide and 20 mm long.

The wide angle X-ray diffraction (WAXD) was measured using an Ni-filtered CuKα radiation generated by a Geiger Flex XGC 20 (Rigaku Co. Ltd). The meridional and equatorial profiles were obtained by the transmission method. The orientation functions, *f*, of the crystal axes was obtained by the azimuthal intensity distribution of the WAXD reflection

$$f = (3\langle\cos^2\phi\rangle - 1)/2$$

where ϕ is the angle between the corresponding crystal axis and the drawing direction. The intensity of the background was measured on the lower and higher angle sides of the reflection, and was subtracted from the intensity of the reflection. The WAXD patterns were taken with an imaging plate camera. The temperature dependence of WAXD was obtained by heating the sample in a hot plate, Mettler FP82HT. The polarized FTIR spectra of the drawn films were measured with a Bio-rad FTS 60A-896 FTIR spectrophotometer, equipped with a wire grid polarizer. Thin films

spin-cast on the quartz plates were used for the measurements of UV absorption spectroscopy. The UV spectra at elevated temperatures were measured using a Shimadzu UV 2500 PC spectrophotometer and a UV cell with a temperature-controlled furnace. The UV spectra at low temperatures were obtained using a UV cell, with a small liquid-nitrogen container and a temperature-controlled heater. The oriented thin films prepared by rubbing a spin-cast film were characterized by the polarized UV absorption spectroscopy. The Glan–Thompson polarizing prism was used for the polarization measurements. The fluorescence spectra were measured with a fluorescence spectrophotometer FP777 (Japan Spectroscopic Co. Ltd).

3. Results and discussion

3.1. Thermal and mechanical properties

Fig. 1 shows DSC curves of drawn films of PDM-*co*-MPS. The samples exhibit a sharp peak at 80–90°C and a broad endotherm in the range of 70–130°C, suggesting that two kinds of structural transitions lie in this temperature range. On the DSC curves of the first heating process, a small peak is observed at 40°C. The peak may originate from poorly ordered crystals in the initial crystalline texture of the as-drawn film. The sharp peak around 86°C is intensified in the second heating process, suggesting a higher crystallinity in the melt-crystallized film than in the as-drawn film. The DSC curves of the 58/42 copolymer are similar to those of the 63/37 copolymer.

Dynamic viscoelasticity of the 58/42 copolymer is shown in Figs. 2 and 3. A large loss tan δ peak is observed at -20 to -10°C, suggesting that structural relaxation occurs in this temperature range. The dynamic storage modulus markedly decreases with the rise in temperature in the range of this transition. There is also a sharp drop of dynamic storage modulus above 60°C, corresponding to the transition observed in the DSC measurements. A small loss tan δ shoulder around 40°C may correspond to the small peak observed on the first heating DSC curve. The dynamic storage modulus of isotropic film is 0.28 GPa at ambient temperature and this value is close to the reported modulus for a film of poly(*n*-pentyl-*n*-alkylsilylene) [11]. The drawn and heat-treated film shows a dynamic storage modulus 3–7 times higher than that of the as-cast film in the temperature range studied. The modulus of the drawn sample is as high as 13.3 GPa at -150°C, but the value is still lower than the crystal modulus (50–60 GPa) of PDMS [12].

3.2. Structure of drawn films

WAXD profiles of drawn films of 58/42 and 63/37 (DM/MP) copolymers are shown in Fig. 4. The values of lattice spacing, *d*, are summarized in Table 2. It is difficult to determine the crystal structure of the copolymers owing to the limited number of reflections. The crystal structures of the copolymers are considered to be different from those of the homopolymers, because the WAXD peak positions of the copolymer neither agree with the peak positions of PDMS nor with those of PMPS. The result suggests that DM and MP units co-crystallize in the common crystal lattice and that the copolymers have a random sequence distribution. The equatorial profile for the 63/37 copolymer is similar to that for the 58/42 copolymer, while the meridional profile is quite different between the copolymers. A sharp meridional reflection is observed at $d = 0.193$ nm for the 58/42 copolymer. As the crystal lattice constant *c* of the copolymer is nearly equal to the value of the homopolymers having all-*trans* conformation [20,21], the conformation of the PDM-*co*-MPS is considered to be all-*trans* in the crystal

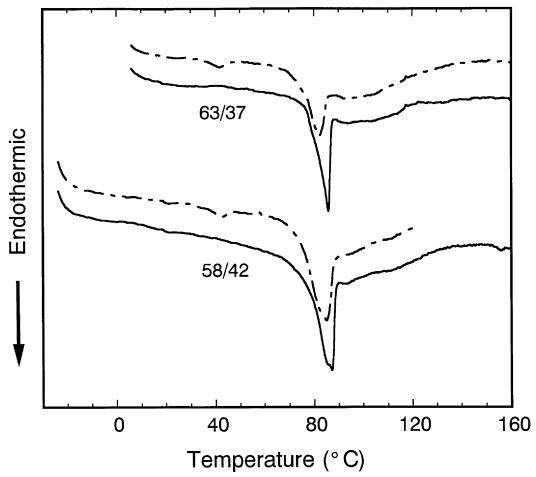

Fig. 1. DSC scans of drawn PDM-*co*-MPS: (– – – –) first heating process; (—) second heating process.

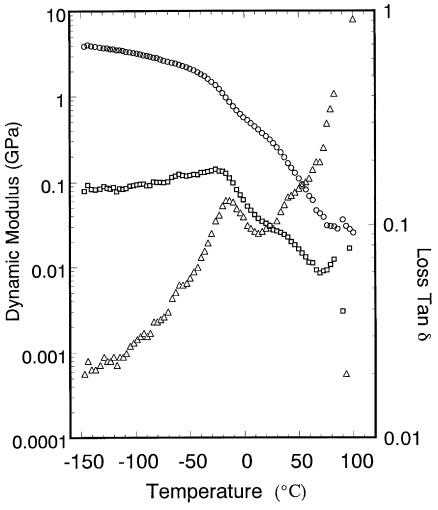

Fig. 2. Dynamic viscoelasticity (35 Hz) of the as-cast film of the 58/42 copolymer: (○) dynamic storage modulus; (□) dynamic loss modulus; (△) loss tan δ.

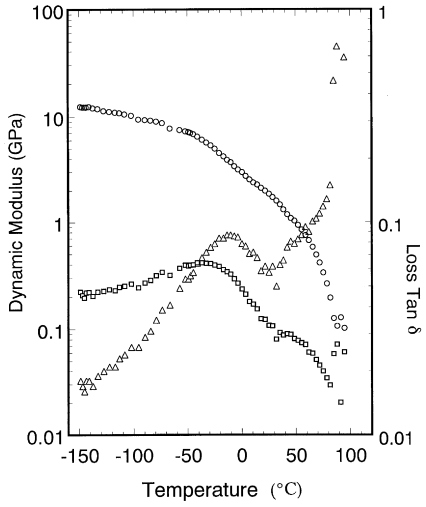

Fig. 3. Dynamic viscoelasticity (35 Hz) of the drawn and annealed sheet of the 58/42 copolymer (draw ratio = 7.5 times, drawing temperature = 70° C): (○) dynamic storage modulus; (□) dynamic loss modulus; (△) loss tan δ.

phase. On the contrary, no meridional reflection is observed in the WAXD profile of the 63/37 copolymer. Although the molecular chains of the 63/37 copolymer pack into the crystal lattice, the periodicity does not form in the direction of the fibre-axis. The orientation functions, f_{hk0} and f_c are obtained from the azimuthal intensity distribution of the equatorial reflection ($d = 0.787$ nm) and the meridional reflection ($d = 0.193$ nm), respectively. The orientation functions, f_{hk0} and f_c represent the degree of crystal orientation of the *hk0*- and *c*-axes, respectively. The orientation

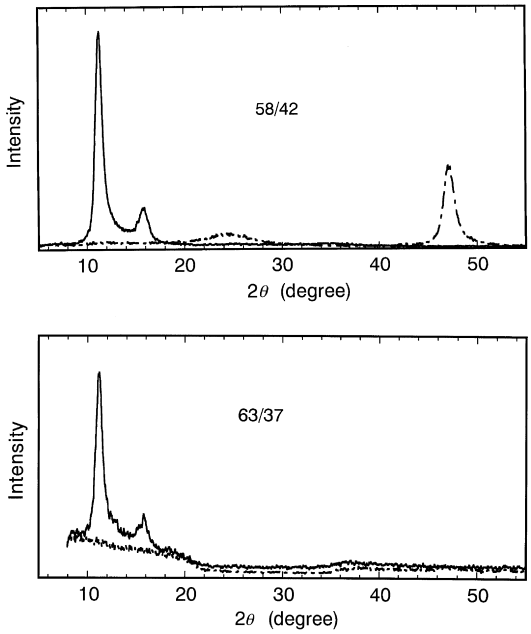

Fig. 4. WAXD profiles of the drawn film of 58/42 copolymer (upper) and the 63/37 copolymer (lower): (—) equatorial scan; (– - – - –) meridional scan.

Table 2
WAXD data of the 58/42 copolymer

2θ (degree)	*d*-Spacing (nm)	
Crystal phase		
11.25	0.787	Equatorial
15.8	0.561	Equatorial
24.8	0.359	First-layer
47.2	0.193	Meridional
Mesophase		
12.0	0.738	Equatorial

functions are summarized in Table 3. The crystal *c*-axis lines up to the drawing direction (DD) and the *hk0*-axis orients perpendicular to DD. The values of orientation function show that the molecular chains in the crystal phase are highly oriented.

The polarized FTIR spectra of the 58/42 copolymer are shown in Fig. 5. The FTIR spectra of the copolymers are approximately a combination of the spectra of the homopolymers in this spectral range. Although the assignment of FTIR spectra has been extensively studied for PDMS homopolymer [22], the assignment of each IR band is not established for PMPS and the copolymers. The absorption band at 1249 cm^{-1} can be assigned to the symmetric CH_3 deformation of the methyl groups directly bonded to the silicon main-chain [22]. This band gives us information on the molecular structure of the entire molecular chains, because it is observed both in the spectra of PDMS and PMPS homopolymers. The orientation function, *f*, of molecular chains is obtained from the dichroic ratio of the 1249 cm^{-1} band:

$$f = [(D - 1)/(D + 2)] \times [(D_0 + 2)/(D_0 - 1)]$$

$$D_0 = 2 \cot^2 \gamma$$

where D is the observed dichroic ratio of the 1249 cm^{-1} band and γ is the transition moment angle with respect to the molecular chain axis. The transition moment of the CH_3 symmetric deformation is parallel to the Si–C bond and is perpendicular to the chain axis ($\gamma = 90°$). The 1249 cm^{-1} band exhibits a large perpendicular dichroism in the polarized FTIR spectra, suggesting the parallel orientation of molecular chains in the drawing direction.

As the 1249 cm^{-1} band originates from both crystal and amorphous regions, the orientation function calculated

Table 3
Orientation functions and dynamic storage modulus at ambient temperature

Sample	E' (GPa)[a]	f_{hk0} (11.3°)	f_c (47.2°)	f_{total}
58/42 (drawn)	1.78	− 0.462	0.943	0.630
58/42 (as-cast)	0.283			
63/37 (drawn)	1.35	− 0.486		0.556
63/37 (as-cast)	0.254			

[a] Dynamic storage modulus at 25°C.

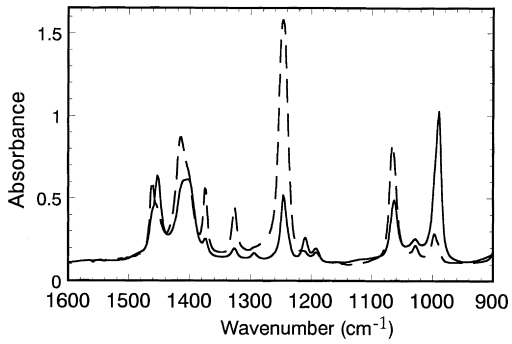

Fig. 5. Polarized FTIR spectra of the drawn 58/42 copolymer: (—) parallel polarization; (– – –) perpendicular polarization.

from the 1249 cm^{-1} band stands for the total orientation function of the molecular chains in both phases. The total orientation function is lower than the crystal orientation function suggesting that the degree of orientation in the amorphous phase is lower than that in the crystal phase. The dynamic storage modulus at ambient temperature is shown in Table 3. The dynamic storage modulus of the drawn film is 5.3–6.3 times higher than that for the as-cast film at 25°C. The molecular orientation is responsible for the increase of modulus. The modulus of the drawn sample of 58/42 copolymer is higher than that for the 63/37 copolymer, and the result is considered to be related to the total orientation function which is higher in the former than in the latter. The modulus of the drawn sample is as high as 13.3 GPa at −150°C, but the value is still lower than the crystal modulus (50–60 GPa) of PDMS. The difference mainly originates from the limited crystallinity and the insufficient orientation in the amorphous phase.

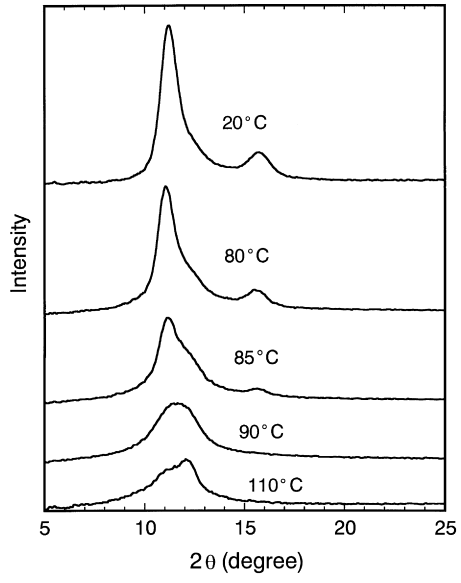

Fig. 6. Temperature dependence of the equatorial scans of the drawn 63/37 copolymer.

Fig. 6 shows the equatorial WAXD profile of the drawn 63/37 copolymer, for which the background scattering is subtracted from the observed profile. The WAXD profile for the 58/42 copolymer is similar to that for the 63/37 copolymer, but the drawn film of the 58/42 copolymer fractured above 90°C. The reflections at $2\theta = 11.25°$ ($d = 0.787$ nm) and $2\theta = 15.8°$ ($d = 0.561$ nm) decrease in intensity and a new reflection appears at $2\theta = 12°$ ($d = 0.738$ nm) with the rise in temperature in the temperature range of 80–90°C. The new reflection originates from the columnar mesophase, in which the conformation of the polymer chain is fairly disordered. A sharp DSC peak at 80–90°C is ascribed to the crystal to columnar mesophase transition. Fig. 7 shows the temperature dependence of the WAXD photograph of the drawn 63/37 copolymer. The molecular orientation is preserved during the crystal–mesophase transition but is gradually randomized with the rise in temperature in the columnar mesophase.

3.3. Thermochromism

Fig. 8 shows the temperature dependence of the UV spectra of the 58/42 copolymer in the first and second heating processes. As-cast film shows an absorption peak at 328 nm, but the peak shifts to 336 nm in the second heating process. The molecular conformation is basically all-*trans* at room temperature, but the Si–Si–Si–Si dihedral angle is considered to be more close to 180° in the melt-crystallized film than in the as-cast film. The analogous results are obtained for 63/37 copolymer, which shows a UV absorption peak at 329 nm and at 333 nm, in the first and second heating processes, respectively. The UV spectrum changes with temperature exhibiting two isoabsorptive points at 315 and 300 nm both in the first and second heating processes. This means that the conformational change occurs in two-steps and that there are three different states of molecular conformation. It is general in polysilanes that the ordered conformation with all-*trans* segment gives rise to light absorption at longer wavelength than the disordered conformation. The first conformation that is stable in the crystal phase is all-*trans* and shows a sharp absorption peak at 328–336 nm. The conformation is fairly disordered in the columnar mesophase (above 85°C). The second conformation, which absorbs at 310–330 nm, is stable in the temperature range of 90–120°C. Above 120°C, an absorption peak due to the third conformation is observed around 300 nm. The third conformation is more disordered with the lower *trans* content than the second conformation. A broad DSC endotherm in the range of 80–140°C is considered to originate from the disordering of conformation in the columnar mesophase.

Fig. 9 shows the polarized UV spectra of the rubbed film of the 58/42 copolymer. The absorbance for the parallel polarization is higher than that for the perpendicular polarization. As the transition dipole moment in the first σ–σ^* transition of polysilanes is parallel to the molecular chain

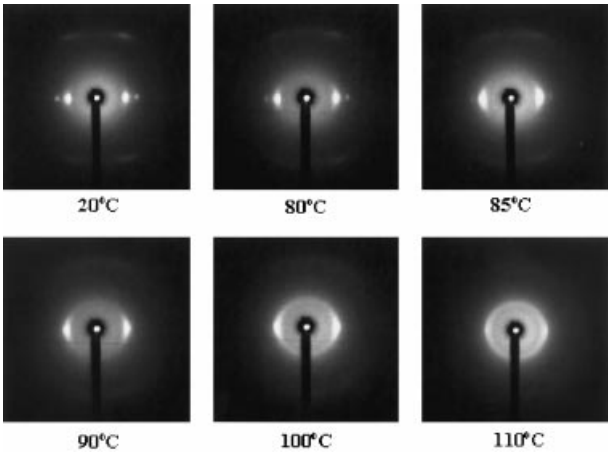

Fig. 7. Temperature dependence of WAXD pattern of the drawn 63/37 copolymer.

direction, the molecular chains are oriented parallel to the rubbing direction. The temperature dependence of the dichroic ratio is shown in Fig. 10. The dichroic ratio starts to decrease at 80–90°C, and approaches zero above 120°C. The randomization of the molecular orientation as well as the disordering of the conformation proceeds with the rise in temperature in the columnar mesophase. The copolymer

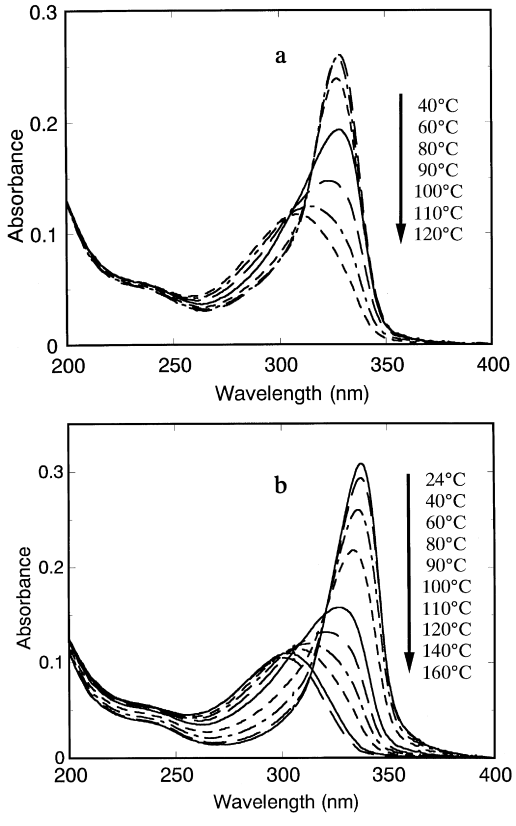

Fig. 8. Temperature dependence of the UV spectra of the 58/42 copolymer: (a) first heating process; (b) second heating process; (—) 24°C; (– – –) 40°C; (– - – - –) 60°C; (- - -) 80°C; (—) 90°C; (– – –) 100°C; (– - – - –) 110°C; (- - -) 120°C; (—) 140°C, (– – –) 160°C.

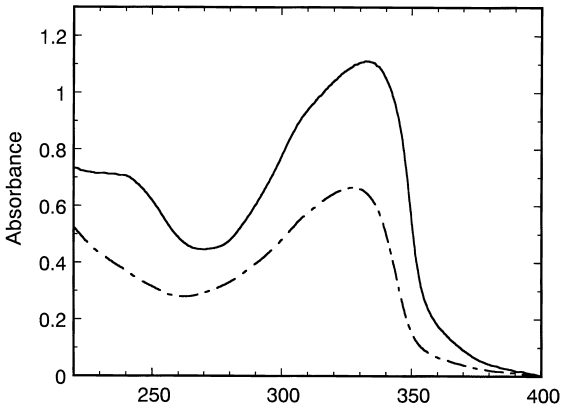

Fig. 9. Polarized UV spectra of the rubbed film of the 58/42 copolymer: (—) parallel polarization; (– - – - –) perpendicular polarization.

film is extensible in the columnar mesophase, but the maximum draw ratio significantly decreases with the rise in temperature. The structural changes of the mesophase would reduce the extensibility of the copolymer films. Although the orientation is almost randomized above 110°C for the 58/42 copolymer, the oriented structure in the mesophase remains at 110°C for the 63/37 copolymer. The intermolecular interaction stabilizes the oriented structure in the mesophase more effectively in the 63/37 copolymer than in the 58/42 copolymer owing to the lower content of *n*-propyl side-chains.

Fig. 11 shows the temperature dependence of UV spectra in the low temperature range. The as-cast film is cooled to −80°C and the UV spectrum is measured in the first heating process. The UV spectrum does not change with temperature, except for the absorbance being lower at −80°C than at higher temperatures. The large tan δ peak is observed at −20°C in the dynamic viscoelasticity (Fig. 2). The low-temperature relaxation does not accompany the conformational change of the silicon main-chains. Therefore, the large loss tan δ peak observed at −20 to −10°C would be

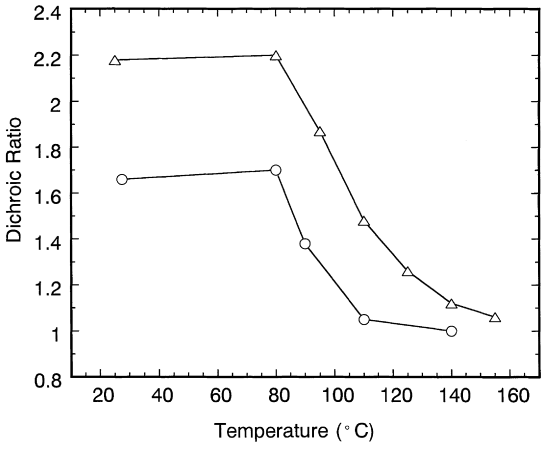

Fig. 10. Temperature dependence of dichroic ratio in the rubbed film: (○) 58/42 copolymer; (△) 63/37 copolymer.

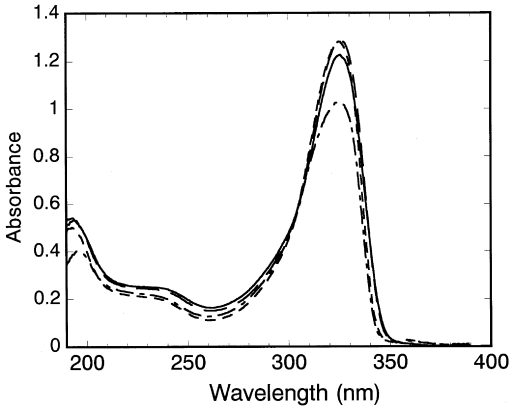

Fig. 11. Temperature dependence of the UV spectra of the 58/42 copolymer in the low temperature region: (– - - - –) −80°C; (- - -) −60°C; (– – –) 5°C; (—) 27°C.

related to the molecular motion of the *n*-propyl group or to the glass transition in the disordered phase.

3.4. Effects of structure on fluorescence spectrum

The polarized fluorescence of the drawn film is shown in Fig. 12. Two emission peaks are observed at 350 and 362 nm. Although the emission peaks at 350 nm is highly polarized, the degree of polarization is low for the emission peak at 362 nm. Fig. 13 shows the effects of thickness and heat treatment on the fluorescence spectrum. Although the thin spin-cast film shows an emission peak at 348 nm, the thick annealed film exhibits a peak at 358 nm. Both of them are observed in the thick as-cast film. The relative intensity of the two emission peaks seems to be affected by the crystallization. The highly polarized emission at 350 nm originates from the σ–σ^* transition of the oriented silicon main-chains. Although the origin for the 360 nm emission peak is not clearly known, the low-energy emission site is considered to be formed in the crystalline texture.

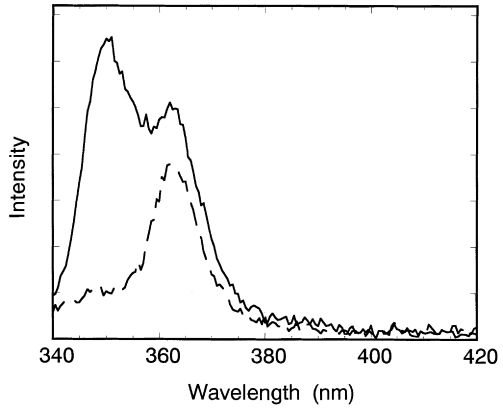

Fig. 12. The polarized fluorescence spectra of the drawn film of the 58/42 copolymer excited at 330 nm: (—) parallel polarized emission; (– –) perpendicular polarized emission.

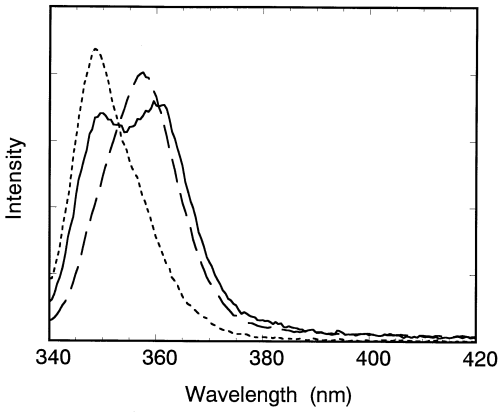

Fig. 13. The fluorescence spectrum: (- - -) spin-cast film (thickness: 220 nm); (—) as-cast film (thickness: 15 μm); (– – –) annealed film (thickness:15 μm).

4. Conclusions

The PDM-*co*-MPS film cast from hexane solution were shown to be drawn to a high elongation (7–8 times) at 70–90°C, at which the crystal–mesophase transition starts to occur. The dynamic storage modulus of the drawn and heat-treated film is 3–7 times higher than that of the as-cast film in the temperature range studied. The molecular chains in the crystal phase highly orient to the drawing direction. The high degree of orientation is responsible for the increase of modulus. The results of DSC and thermochromism suggest that two types of structural transitions exist above 80°C. The first transition is the crystal–columnar mesophase transition, and the second one involves the disordering of conformation and the randomization of molecular orientation in the mesophase. The copolymer is extensible only in the narrow temperature range, in which polymer chains are mobile enough but the intermolecular interaction stabilizes the oriented structure so as to transmit the tensile force. The two emission peaks are observed in the fluorescence spectrum. The peak at higher energy is assigned to the σ–σ^* transition of the oriented molecular chains, and the low energy one originates from the other emission site localized in the crystalline texture.

Acknowledgements

Authors express their thanks to Dr Kazuo Nakayama of National Institute of Materials and Chemical Research for the measurements of dynamic viscoelasticity and stimulating discussions.

References

[1] Miller RD, Michl J. Chem Rev 1989;89:1359.
[2] Kepler RG, Zeigler JM, Harrah LA, Kurtz SR. Phys Rev B 1987;35:2818.

[3] Miller RD, Wallraff G, Clecak N, Soriyakumaran R, Michl J, Karatsu AJ, Mckinley AJ, Klingensmith KA, Downing J. Polym Engng Sci 1989;29:882.
[4] Kani R, Nakano Y, Yoshida H, Mikoshiba S, Hayase S. J Polym Sci Polym Chem 1997;35:2355.
[5] Kabeta K, Wakamatsu S, Sugi S, Imai T. Synth Met 1996;82:201.
[6] Fukushima M, Hamada Y, Tabei E, Aramata M, Mori S, Yamamoto Y. Chem Lett 1988:347.
[7] Suzuki H, Meyer H, Hoshino S, Haarer D. J Appl Phys 1995;78:2684.
[8] Ebihara K, Koshihara S, Miyazawa T, Kira M. Jpn J Appl Phys 1996;35:L1278.
[9] Xu Y, Fujino T, Naito H, Oka K, Dohmaru T. Chem Lett 1998:299.
[10] Yuan C-H, Hoshino S, Toyoda S, Suzuki H, Fujiki M, Matsumoto N. Appl Phys Lett 1997;71:3326.
[11] Klemann BM, DeVilbiss T, Koutsky JA. Polym Engng Sci 1996;36:135.
[12] Shimomura M, Yatabe T, Kaito A, Tanabe Y. Macromolecules 1997;30:5570.
[13] Kyotani H, Tanigaki N, Minami N. Polym Prepr Jpn 1995;44:1543.
[14] Wesson JP, Willams TC. J Polym Sci Polym Chem Ed 1980;18:959.
[15] Frey H, Matyjaszewski K, Moeller M, Oelfin D. Colloid Polym Sci 1991;269:442.
[16] Schilling FC, Lovinger AJ, Davis DD, Bovey FA, Zeigler JM. Macromolecules 1992;25:2854.
[17] Schilling FC, Lovinger AJ, Davis DD, Bovey FA, Zeigler JM. Macromolecules 1993;26:2716.
[18] Menescal R, Eveland J, West R, Leites LL, Bukalov SS, Yadriseva TD, Blazso M. Macromolecules 1994;27:5885.
[19] Out GJJ, Turetskii AA, Moeller M, Oelfin D. Macromolecules 1995;28:596.
[20] Lovinger AJ, Davis DD, Scilling FC, Padden Jr FJ, Bovey FA, Zeigler JM. Macromolecules 1991;24:132.
[21] Jambe B, Janos A, Devaux J. Polymer 1996;37:1533.
[22] Leites LA, Bukoalov SS, Yadritzeva TS, Mokhov MK, Antipova BA, Frunze TM, Dementev VV. Macromolecules 1992;25:2991.